Electronic Supplementary Material (ESI) for Physical Chemistry Chemical Physics.

Supplementary Data

Interfacial Water Effect on Cooperativity and Signal Communication in *Scapharca* Dimeric Hemoglobin

Sheh-Yi Sheu,[a,b,†,*] Yu-Cheng Liu[b] and Dah-Yen Yang[c,†,*]

[a]Department of Life Sciences, Institute of Genome Sciences and [b]Institute of Biomedical informatics, National Yang-Ming University, Taipei 112, Taiwan

[c]Institute of Atomic and Molecular Sciences, Academia Sinica, Taipei 106, Taiwan

Table S1: Bending and twisting moduli of the HbI protein

Helix	**Type I**				**Type II**				**Type III**			
	Amer		Bmer		Amer		Bmer		Amer		Bmer	
	bend[a]	twist[a]	bend	twist	bend	twist	bend	twist	bend	twist	bend	twist
A	669.6	367.9	681.1	349.3	654.2	364.5	548.0	340.8	676.1	350.3	654.2	362.1
B	733.5	363.1	747.4	371.7	738.7	402.8	721.5	399.5	736.2	400.9	738.7	402.9
E	768.3	426.4	774.4	435.9	952.7	415.6	945.2	422.3	980.3	454.1	953.3	420.2
F	649.6	386.0	677.8	366.2	642.4	402.2	669.3	401.9	663.2	407.5	626.0	425.9
G	723.7	432.1	753.0	422.6	746.6	424.2	728.9	431.3	746.6	413.5	730.4	426.1
H	650.0	473.9	657.7	452.3	701.2	435.4	684.8	431.3	665.4	457.6	665.6	434.5

[a] Bend and twist moduli are in unit pN/Å.

Table S2: List of three cases and two simulation methods

Case	I		II		III	
Subunit	Amer	Bmer	Amer	Bmer	Amer	Bmer
Simulation method	MD (2 ns)	MD (2 ns)	TMD (500 ps) + MD (8 ns)	MD (8.5 ns)	TMD (500 ps)	TMD (500 ps)

Table S3: Definition of the secondary structure index in the cross-correlation analysis

Segment ID	Secondary structure index	Residue ID	Secondary structure	Helix index
Amer/Bmer	1	3-8	helix	A’
Amer/Bmer	2	9-11	loop	
Amer/Bmer	3	12~25	helix	A
Amer/Bmer	4	26~28	loop	
Amer/Bmer	5	29~43	helix	B
Amer/Bmer	6	44	loop	
Amer/Bmer	7	45~54	helix	C
Amer/Bmer	8	55-56	loop	
Amer/Bmer	9	57-62	helix	D
Amer/Bmer	10	63	loop	
Amer/Bmer	11	64-82	helix	E
Amer/Bmer	12	83-86	loop	
Amer/Bmer	13	87-102	helix	F
Amer/Bmer	14	103-107	loop	
Amer/Bmer	15	108-111	helix	G’
Amer/Bmer	16	112-113	loop	
Amer/Bmer	17	114-124	helix	G
Amer/Bmer	18	125-128	loop	
Amer/Bmer	19	129-144	helix	H
Amer/Bmer	20	hemeA	loop	

Table S4: Signal transduction pathways

Pathway	Query	Reference
Intra-subunit		
1	AA', AA, AB	AD, AE, AF
2	AA', AA, AB, AC	AG', AG, AH
3	AD, AE, AF	AG, AH
4	BA', BA, BB	BD, BE, BF
5	BA', BA, BB, BC	BG', BG, BH
6	BE, BF, BG	BG, BH
Inter-subunit		
7	AA, AB	BA', BA, BB
8	AA', AA, AB	BD, BE, BF
9	AB	BG', BG, BH
10	AC, AD, AE	BA', BA, BB
11	AD, AE, AF	BD, BE, BF
12	AD, AE	BG', BG, BH
13	AG, AH	BA', BA
14	AG, AH	BD, BE, BF

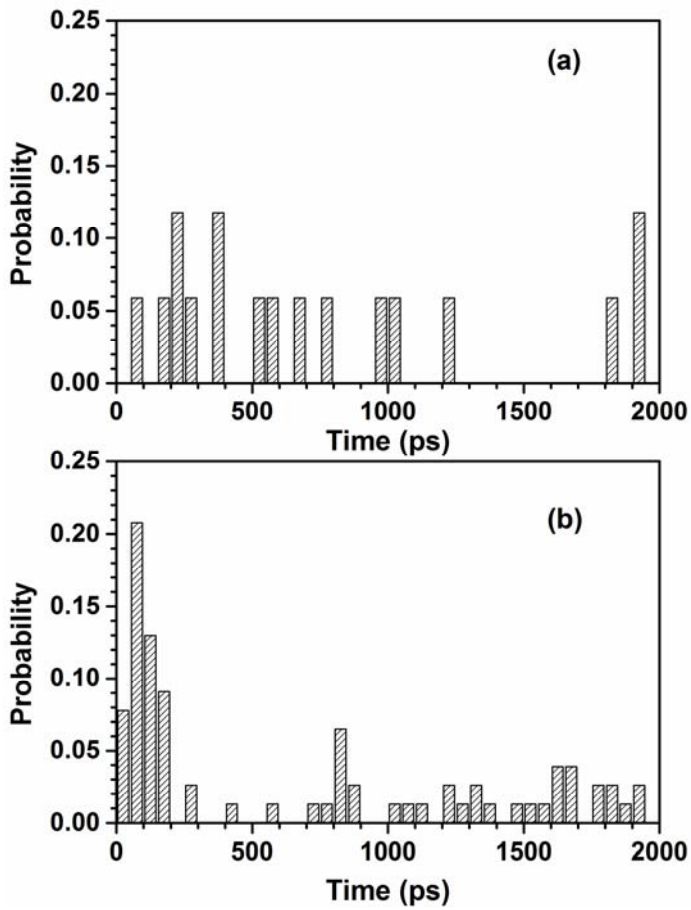

Figure S1. The Phe97 χ_1 flipping time distribution. Two systems are: (a) the NIW system and (b) the WIW system.

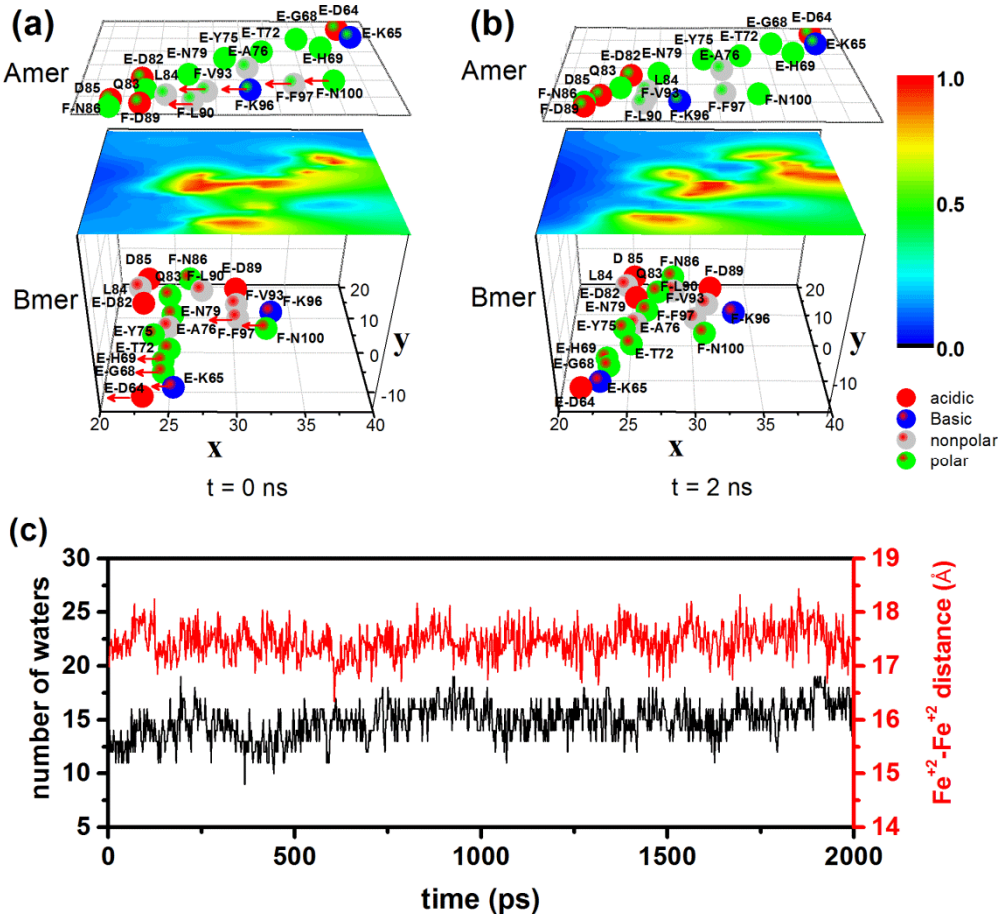

Figure S2. Projection of the interface region. Initially, HbI is unligated at the oxy-state, followed by a 2-ns MD simulation, where the structure of HbI changes gradually toward the deoxy-state. (a) MD time t = 0 and (b) t = 2 ns. The interface residues in Amer and Bmer and the density of interfacial water molecules are projected on the upper, lower and middle panels, respectively. The acidic (red), basic (blue), nonpolar (grey) and polar (green) residues are shown in colored-ball representation. In (a), a red arrow indicates the residue movement from t = 0 to 2 ns. Explicitly, the residues of the AF-helix (BE-helix) move toward the residues of AE-helix (BF-helix). This is EF helix hinge motion.[1] (c) The number of water molecules and the Fe^{+2}-Fe^{+2} distance versus MD time.

Type	I	II	III
(a)	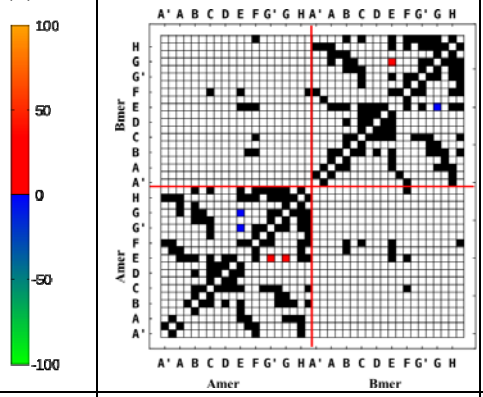	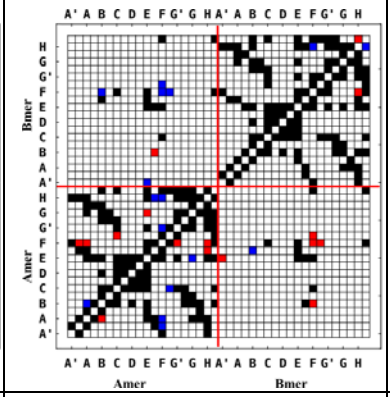	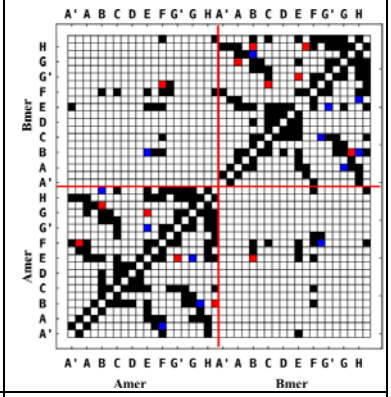
(b)	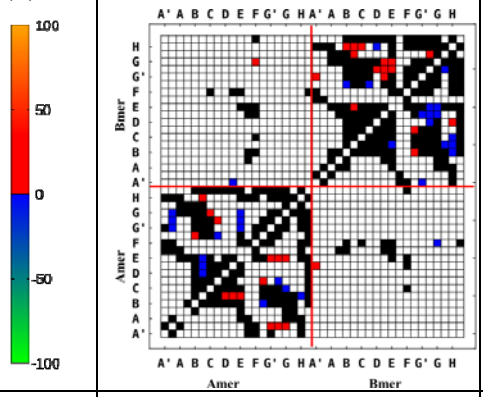	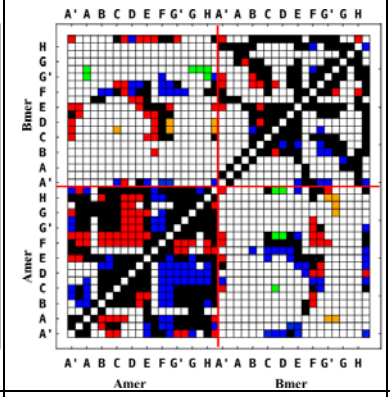	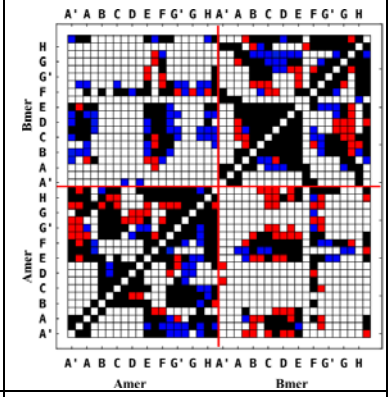
(c)	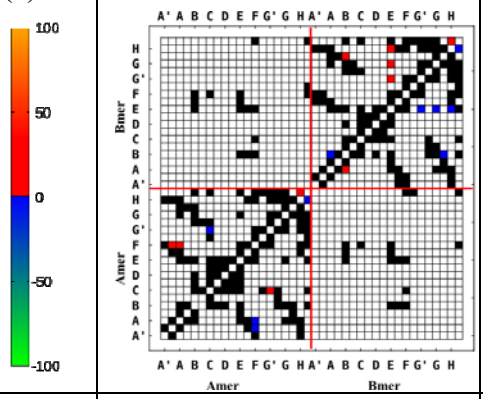	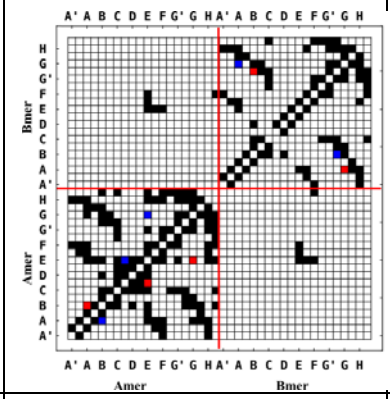	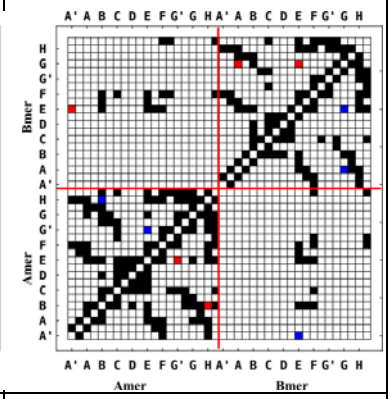
(d)	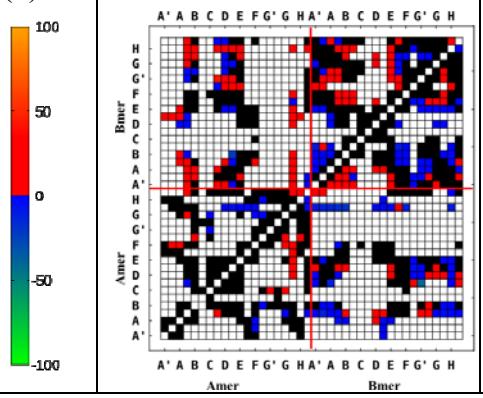	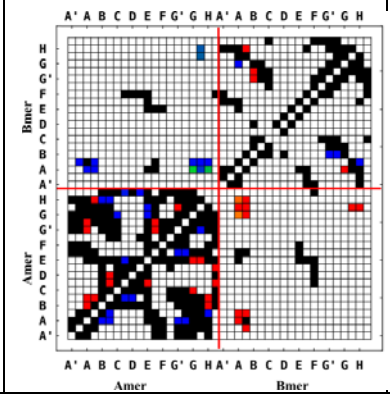	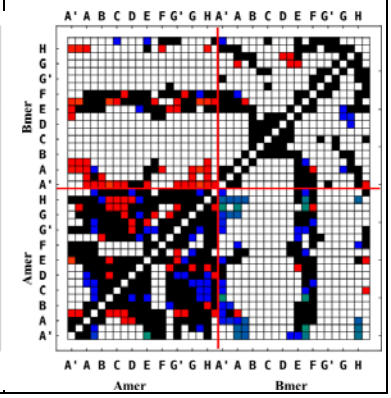

Figure S3. Communication map of the signal transduction. Three RMSF types, I, II and III, in the NIW system (a) with contact and (b) the overall correlation and in the WIW system (c) with contact and (d) the overall correlation. The correlation is shown for correlation coefficients > 0.5 and at contact distances < 3.5 Å. The spectrum scale is marked in units of ps.

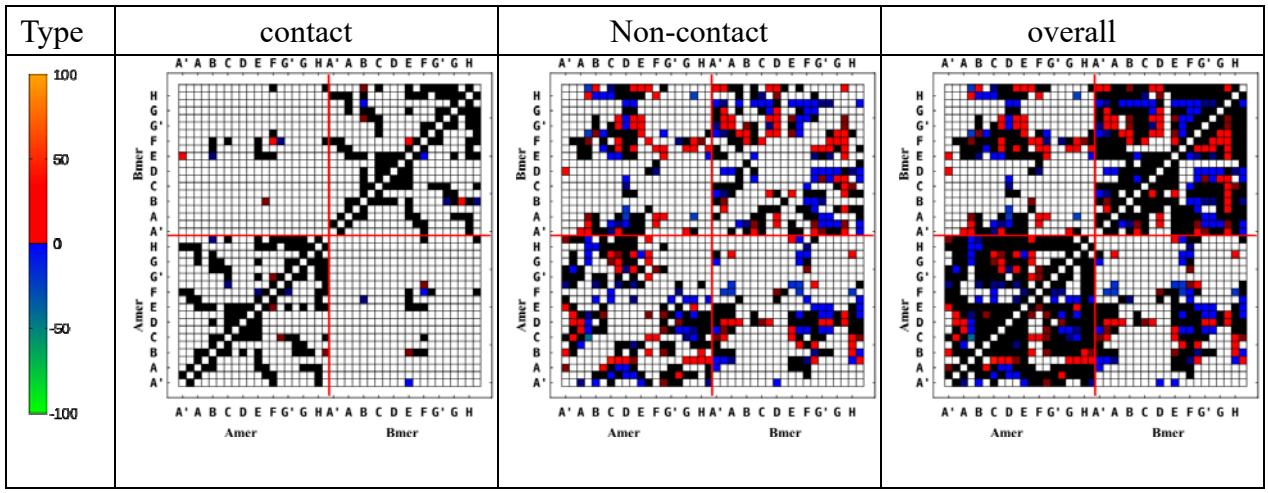

Figure S4. Communication map of the signal transduction based on the TMD trajectory in the WIW system. After TMD simulation, the structural transition occurs from the oxy-state to the deoxy-state. The correlation is shown for correlation coefficients > 0.5 and at contact distances < 3.5 Å. The spectrum scale is marked in units of ps. The definition is the same as that shown in the legend to Figure 8.

Theory

Model of the ligand escape process

In general, cooperative behavior correlates the ligand escape process with the gate opening function, which is controlled by protein dynamic motions. Thus, the time-dependent gate function dominates the ligand escape time. Here, we consider the escape process of a Brownian particle from a spherical continuous model with a reflection wall and an arbitrary gating function;[2] the model is geometric, and the gate function is time-dependent and entropy-driven (**Figure S5a**). Inside the spherical cavity, there is an entropic potential, such as one based on geometric entropy, and the ligand is initially located at the center. On the cavity surface, there is a hole that acts as a gate, whose undulation is regulated by protein dynamics. The ligand diffuses with a diffusion constant D_0 inside the cavity and is reflected from the wall until it reaches the gate. For a perfect absorption gate (i.e., $\nu \to \infty$, where $\nu = k_0/(4\pi D_0 R^2)$ and k_0 is the reaction rate), the survival time τ_0 of ligand escape from the cavity can be expressed as

$$\tau_0 = -\frac{1}{2\sqrt{2}\,\pi} \mathrm{Re}[\,\tilde{F}_0^{-1}\,]\, n_0^0(R) \qquad (1)$$

where $\widetilde{F}_0^{-1}$ describes the gating effect and is the Fourier transform of the gate function, $F(t) = \frac{1}{\nu} H^{-1}(\theta(t) - \theta)$, $H^{-1}(\theta(t) - \theta)$ is the inverse of the step function, $\theta(t)$ is the gate function expressed as a polar angle, and $n_0^0(R)$ describes the surface diffusion motion on the cavity surface.

Correspondingly, the ligand escape process inside a gated cavity can be described as a Brownian particle moving on an entropy potential, $\bar{U} = V + U$, where $V = -k_B T \ln (r/R)^2$ and $U = -k_B T \ln \sin\theta$ (**Figure S5b**). Here, *r* is the distance from the cavity center, *R* is the radius of the cavity, k_B is the Boltzmann constant, and T is the temperature. Note that this entropy potential is decomposable, and two singularities are present, at $\theta \to 0$ and π. Then, it is straightforward to confirm that the gate closes at $\theta \to 0$, defined as the spot, thus providing a high barrier to ligand escape. The Brownian particle moves on this entropy potential, starting from a position (r, θ) = (0, $\pi/2$), until it reaches the gate.

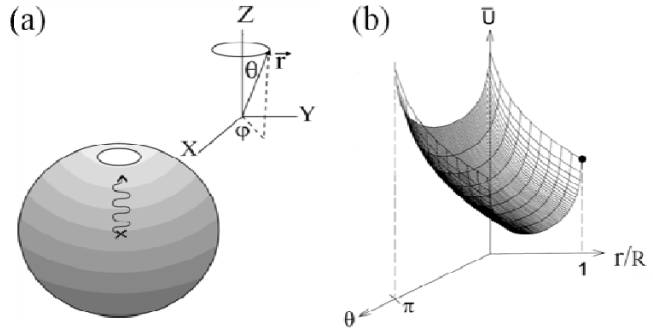

Figure S5. Model of the ligand escape theory. (a) The top gate (punctured hole) is a function of azimuth angle θ along the z-axis presented as spherical coordinates. (b) The entropy potential surface inside a 3D-ball. An entropy potential can be expressed in terms of (r, θ). In particular, the gate is located at (R, 0), and the ligand is located initially at (0, $\pi/2$).

1 Z. Ren, V. Šrajer, J. E. Knapp and W. E. Royer, *Proc. Natl. Acad. Sci. U. S. A.*, 2012, **109**, 107-112.

2 S.-Y. Sheu and D.-Y. Yang, *J. Chem. Phys.*, 2000, **112**, 408-415.